

# Concurrent Constant Modulus Algorithm and Soft Decision Directed Scheme for Fractionally-Spaced Blind Equalization

S. Chen<sup>†</sup> and E.S. Chng<sup>‡</sup>

<sup>†</sup> School of Electronics and Computer Science  
University of Southampton, Southampton SO17 1BJ, U.K.

<sup>‡</sup> School of Computer Engineering  
Nanyang Technological University, Singapore 639798

## ABSTRACT

The paper proposes a concurrent constant modulus algorithm (CMA) and soft decision-directed (SDD) scheme for low-complexity blind equalization of high-order quadrature amplitude modulation channels. Simulation using a fractionally-spaced equalization setting is used to compare the proposed scheme with the recently introduced state-of-art concurrent CMA and decision-directed (DD) scheme. The proposed CMA+SDD blind equalizer is shown to have simpler computational complexity per weight update, faster convergence speed, and slightly improved steady-state equalization performance, compared with the CMA+DD blind equalizer.

## I. INTRODUCTION

For communication systems employing high bandwidth-efficiency quadrature amplitude modulation (QAM) signalling, the constant modulus algorithm (CMA) based equalizer is by far the most popular blind equalization scheme [1]–[4]. It has very simple computational requirements and readily meets the real-time computational constraint. The CMA is also very robust to imperfect carrier recovery. A particular problem of the CMA, however, is that it only achieves a moderate level of mean square error (MSE) after convergence, which may not be sufficiently low for the system to obtain adequate performance. A possible solution is to switch to a decision directed (DD) adaptation which should be able to minimize the residual CMA steady state MSE [5]. However, as pointed out in [6], in order for such a transfer to be successful, the CMA steady state MSE should be sufficiently low. In practice, such a low level of MSE may not always be achievable by the CMA.

De Castro and co-workers [6] have suggested an interesting solution to this problem. Rather than switching to a DD adaptation after the CMA has converged, they have proposed to operate a DD equalizer concurrently with a CMA equalizer. To avoid error propagation due to incorrect decisions, the DD weight adaptation only takes place if the CMA adaptation is judged to have achieved a successful adjustment with high probability. At a cost of slightly more than doubling the complexity of the very simple CMA, this concurrent CMA+DD equalizer is reported to obtain a dramatical improvement in equalization performance over the CMA [6], and it represents a state-of-art technique for low-complexity blind equalization of high-order QAM channels. Another blind equalization scheme, which is relevant to the proposed concurrent CMA and soft decision-directed (SDD) blind equalizer, is the bootstrap maximum *a posteriori* probability (MAP) blind equalizer [7],[8].

The bootstrap MAP blind scheme was originally derived in [9] for the 4-QAM case and extended to  $M$ -QAM channels in [7],[8],

and it has been shown to outperform the CMA+DD scheme, in terms of convergence rate and steady-state performance [10],[11]. A drawback of this bootstrap MAP scheme is that its adaptive process requires  $L$ -stage switchings, where  $L = \log_2(M)/2$ , and each stage of adaptation needs a different set of algorithm parameters. Thus, tuning of the bootstrap MAP algorithm is quite complicated. The proposed CMA+SDD scheme may be viewed as operating a CMA equalizer and a last-stage bootstrap MAP equalizer concurrently, and it does not require complicated switching. The proposed CMA+SDD scheme has a simpler complexity than the CMA+DD scheme. Simulation results obtained under a fractionally-spaced equalizer (FSE) setting show that the CMA+SDD algorithm has a faster convergence rate and slightly better steady-state performance, compared with the CMA+DD scheme.

## II. LOW-COMPLEXITY BLIND EQUALIZATION

Blind equalization with a  $T_s/2$ -spaced FSE is considered, where  $T_s$  denotes the symbol period. The baseband discrete-time model of communication system with a  $T_s/2$ -spaced FSE [12] is depicted in Fig. 1. For notational convenience, the index  $k$  is reserved for  $T_s$ -spaced quantities and index  $n$  for  $T_s/2$ -spaced quantities throughout the discussion. The transmitted  $T_s$ -spaced complex symbol sequence  $s(k) = s_R(k) + js_I(k)$  is assumed to be independently identically distributed (i.i.d.) and the symbol constellation is  $M$ -QAM with the set of all the symbol points defined by

$\mathcal{S} = \{s_{il} = (2i - Q - 1) + j(2l - Q - 1), 1 \leq i, l \leq Q\}$  (1)  
where  $Q = \sqrt{M} = 2^L$ , and  $L$  is an integer. The received  $T_s/2$ -spaced signal sample is

$$\bar{r}(n) = \sum_{i=0}^{2N_c-1} \bar{a}_i \bar{s}(n-i) + \bar{e}(n) \quad (2)$$

where the  $T_s/2$ -spaced sequence  $\{\bar{s}(n)\}$  is a zero-filled version of the transmitted symbol sequence  $\{s(k)\}$  defined by

$$\bar{s}(n) = \begin{cases} s(n/2), & \text{for even } n, \\ 0, & \text{for odd } n, \end{cases} \quad (3)$$

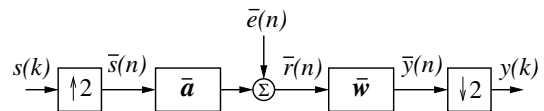


Fig. 1. Multirate baseband model of communication system with  $T_s/2$ -spaced equalizer, where  $T_s$  denotes symbol period, the index  $k$  indicates  $T_s$ -spaced quantities and index  $n$  indicates  $T_s/2$ -spaced quantities.

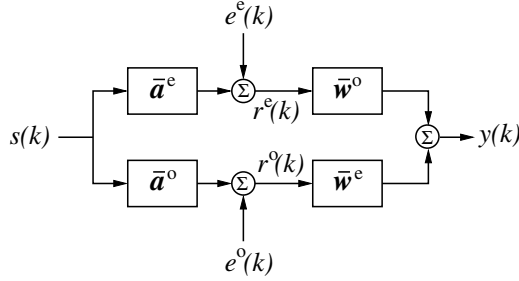


Fig. 2. Multichannel model of communication system with  $T_s/2$ -spaced equalizer, where  $T_s$  denotes symbol period, and the index  $k$  indicates  $T_s$ -spaced quantities.

the channel is specified by the  $T_s/2$ -spaced complex-valued channel impulse response (CIR) given by

$$\bar{\mathbf{a}} = [\bar{a}_0 \bar{a}_1 \bar{a}_2 \bar{a}_3 \cdots \bar{a}_{2N_c-1}]^T \quad (4)$$

with  $N_c$  corresponding to the  $T_s$ -spaced CIR length, and the  $T_s/2$ -spaced sample  $\bar{e}(n) = \bar{e}_R(n) + j\bar{e}_I(n)$  is an i.i.d. complex Gaussian white noise with  $E[\bar{e}_R^2(n)] = E[\bar{e}_I^2(n)] = \sigma_e^2$ .

To remove the channel distortion, a  $T_s/2$ -spaced equalizer is employed, which is defined by

$$\bar{y}(n) = \sum_{i=0}^{2m-1} \bar{w}_i \bar{r}(n-i) = \bar{\mathbf{w}}^T \bar{\mathbf{r}}(n) \quad (5)$$

where  $2m$  is the order or length of the  $T_s/2$ -spaced equalizer,  $\bar{\mathbf{w}} = [\bar{w}_0 \bar{w}_1 \cdots \bar{w}_{2m-1}]^T$  is the equalizer complex-valued weight vector, and  $\bar{\mathbf{r}}(n) = [\bar{r}(n) \bar{r}(n-1) \cdots \bar{r}(n-2m+1)]^T$  is the equalizer input vector. The FSE output  $\bar{y}(n)$  is decimated by a factor of 2 to create the  $T_s$ -spaced output  $y(k)$ . It can easily be shown [12] that the system model of Fig. 1 is equivalent to the model depicted in Fig. 2 by defining

$$\bar{\mathbf{a}}^e = [\bar{a}_0 \bar{a}_2 \cdots \bar{a}_{2N_c-2}]^T, \quad \bar{\mathbf{a}}^o = [\bar{a}_1 \bar{a}_3 \cdots \bar{a}_{2N_c-1}]^T, \quad (6)$$

$$\bar{\mathbf{w}}^e = [\bar{w}_0 \bar{w}_2 \cdots \bar{w}_{2m-2}]^T, \quad \bar{\mathbf{w}}^o = [\bar{w}_1 \bar{w}_3 \cdots \bar{w}_{2m-1}]^T$$

and

$$\begin{aligned} e^e(k) &= \bar{e}(2n), \quad e^o(k) = \bar{e}(2n+1), \\ r^e(k) &= \bar{r}(2n), \quad r^o(k) = \bar{r}(2n+1). \end{aligned} \quad (7)$$

Further define

$$\mathbf{w} = [w_0 w_1 \cdots w_{2m-1}]^T = [(\bar{\mathbf{w}}^o)^T \quad (\bar{\mathbf{w}}^e)^T]^T \quad (8)$$

$$\begin{aligned} \mathbf{r}(k) &= [r(k) r(k-1) \cdots r(k-2m+1)]^T \\ &= [(\mathbf{r}^e(k))^T \quad (\mathbf{r}^o(k))^T]^T \end{aligned} \quad (9)$$

with  $\mathbf{r}^e(k) = [r^e(k) r^e(k-1) \cdots r^e(k-m+1)]^T$  and  $\mathbf{r}^o(k) = [r^o(k) r^o(k-1) \cdots r^o(k-m+1)]^T$ . Then the  $T_s$ -spaced equalizer output  $y(k)$  is given by

$$y(k) = \sum_{i=0}^{2m-1} w_i r(k-i) = \mathbf{w}^T \mathbf{r}(k). \quad (10)$$

### A. Concurrent CMA and decision directed equalizer

De Castro and co-workers [6] proposed a blind equalization scheme that consists of a CMA equalizer and a DD equalizer operating concurrently. Specifically, let  $\mathbf{w} = \mathbf{w}_c + \mathbf{w}_d$ . Here  $\mathbf{w}_c$  is the weight vector of the CMA equalizer which is designed to minimize the CMA cost function

$$\bar{J}_{\text{CMA}}(\mathbf{w}) = E \left[ (|y(k)|^2 - \Delta_2)^2 \right] \quad (11)$$

using a stochastic gradient algorithm, where  $\Delta_2$  is a real positive constant defined by  $\Delta_2 = E[|s(k)|^4] / E[|s(k)|^2]^2$ , while  $\mathbf{w}_d$  is the weight vector of the DD equalizer which is designed to minimize the decision based MSE

$$\bar{J}_{\text{DD}}(\mathbf{w}) = \frac{1}{2} E [|\mathcal{Q}[y(k)] - y(k)|^2] \quad (12)$$

by adjusting  $\mathbf{w}_d$ , where  $\mathcal{Q}[y(k)]$  denotes the quantized equalizer output defined by

$$\mathcal{Q}[y(k)] = \arg \min_{s_{il} \in \mathcal{S}} |y(k) - s_{il}|^2. \quad (13)$$

More precisely, at symbol-spaced sample  $k$ , given

$$y(k) = \mathbf{w}_c^T(k) \mathbf{r}(k) + \mathbf{w}_d^T(k) \mathbf{r}(k), \quad (14)$$

the CMA part adapts  $\mathbf{w}_c$  according to the rule

$$\left. \begin{aligned} \epsilon(k) &= y(k) (\Delta_2 - |y(k)|^2) \\ \mathbf{w}_c(k+1) &= \mathbf{w}_c(k) + \mu_c \epsilon(k) \mathbf{r}^*(k) \end{aligned} \right\} \quad (15)$$

where  $\mu_c$  is a small positive adaptive gain and  $\mathbf{r}^*(k)$  is the complex conjugate of  $\mathbf{r}(k)$ . The DD adaptation follows immediately after the CMA adaptation but it only takes place if the CMA adjustment is viewed to be a successful one. Let

$$\tilde{y}(k) = \mathbf{w}_c^T(k+1) \mathbf{r}(k) + \mathbf{w}_d^T(k) \mathbf{r}(k). \quad (16)$$

Then the DD part adjusts  $\mathbf{w}_d$  according to [6]:

$$\mathbf{w}_d(k+1) = \mathbf{w}_d(k) + \mu_d \delta (\mathcal{Q}[\tilde{y}(k)] - \mathcal{Q}[y(k)]) (\mathcal{Q}[y(k)] - y(k)) \mathbf{r}^*(k) \quad (17)$$

where  $\mu_d$  is the adaptive gain of the DD equalizer and the indicator function

$$\delta(x) = \begin{cases} 1, & x = 0 + j0, \\ 0, & x \neq 0 + j0. \end{cases} \quad (18)$$

It can be seen that  $\mathbf{w}_d$  is updated only if the equalizer hard decisions before and after the CMA adaptation are the same. A potential problem of (hard) decision-directed adaptation is that if the decision is wrong, error propagation occurs which subsequently degrades equalizer adaptation. As analyzed in [6], if the equalizer hard decisions before and after the CMA adaptation are the same, the decision probably is a right one. The DD adaptation, when is safe to perform, has a much faster convergence speed and is capable of lowering the steady state MSE, compared with the pure CMA. The adaptive gain  $\mu_d$  for the DD equalizer can often be chosen much larger than  $\mu_c$  for the CMA. The complexity of this CMA+DD blind equalizer is compared with that of the CMA in Table I.

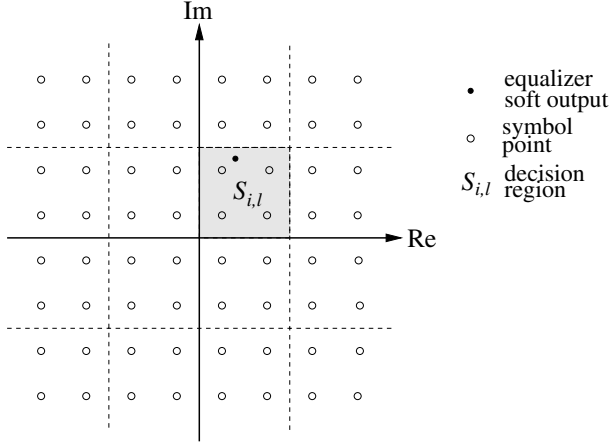


Fig. 3. Illustration of local decision regions for soft decision-directed adaptation with 64-QAM constellation.

### B. Concurrent CMA and soft decision directed equalizer

After the equalization is accomplished, the equalizer soft output  $y(k)$  can approximately be expressed in two terms:

$$y(k) \approx x(k) + v(k) \quad (19)$$

where  $x(k) = s(k - k_d)$ ,  $k_d$  is an integer, and  $v(k) = v_R(k) + jv_I(k)$  is approximately a Gaussian white noise. Thus, if the equalizer weights have correctly been chosen, the equalizer output can be modelled approximately by  $M$  Gaussian clusters with the cluster means being  $s_{il}$  for  $1 \leq i, l \leq Q$ . All the clusters have an approximate covariance

$$\begin{bmatrix} E[v_R^2(k)] & E[v_R(k)v_I(k)] \\ E[v_I(k)v_R(k)] & E[v_I^2(k)] \end{bmatrix} \approx \begin{bmatrix} \rho & 0 \\ 0 & \rho \end{bmatrix}. \quad (20)$$

Under the above conditions, the *a posteriori* probability density function (p.d.f.) of  $y(k)$  is approximately

$$p(\mathbf{w}, y(k)) \approx \sum_{q=1}^Q \sum_{l=1}^Q \frac{p_{ql}}{2\pi\rho} \exp\left(-\frac{|y(k) - s_{ql}|^2}{2\rho}\right), \quad (21)$$

where  $p_{ql}$  are the *a priori* probabilities of  $s_{ql}$ ,  $1 \leq q, l \leq Q$ , and they are all equal.

The computation of the p.d.f. (21) involves the evaluation of  $M \exp(\bullet)$  function values. A local approximation can be adopted for this p.d.f. which only evaluates four  $\exp(\bullet)$  function values. This is achieved by dividing the complex plane into  $M/4$  regular regions, as illustrated in Fig. 3. Each region  $S_{i,l}$  contains four symbol points

$$S_{i,l} = \{s_{pq}, p = 2i - 1, 2i, q = 2l - 1, 2l\}. \quad (22)$$

If the equalizer output  $y(k)$  is within the region  $S_{i,l}$ , a local approximation to the *a posteriori* p.d.f. of  $y(k)$  is

$$\hat{p}(\mathbf{w}, y(k)) \approx \sum_{p=2i-1}^{2i} \sum_{q=2l-1}^{2l} \frac{1}{8\pi\rho} \exp\left(-\frac{|y(k) - s_{pq}|^2}{2\rho}\right) \quad (23)$$

where each *a priori* probability has been set to  $\frac{1}{4}$ . Obviously this approximation is only valid when the equalization goal has been

TABLE I  
COMPARISON OF COMPUTATIONAL COMPLEXITY PER WEIGHT UPDATE. THE EQUALIZER ORDER IS  $2m$ .

equalizer	multiplications	additions	$\exp(\bullet)$
CMA	$8 \times 2m + 6$	$8 \times 2m$	—
CMA+DD	$16 \times 2m + 8$	$20 \times 2m$	—
CMA+SDD	$12 \times 2m + 29$	$14 \times 2m + 21$	4

accomplished. A bootstrap optimization process however can be performed to achieve the MAP solution, as is presented in [7],[8].

The proposed scheme operates a CMA equalizer and a SDD equalizer concurrently. The CMA part is identical to that of the concurrent CMA and DD scheme. The SDD equalizer is designed to maximize log of the local *a posteriori* p.d.f. criterion

$$\bar{J}_{\text{LMAP}}(\mathbf{w}) = E[J_{\text{LMAP}}(\mathbf{w}, y(k))] \quad (24)$$

by adjusting  $\mathbf{w}_d$  using a stochastic gradient algorithm, where

$$J_{\text{LMAP}}(\mathbf{w}, y(k)) = \rho \log(\hat{p}(\mathbf{w}, y(k))). \quad (25)$$

Specifically, the SDD equalizer adapts  $\mathbf{w}_d$  according to

$$\mathbf{w}_d(k+1) = \mathbf{w}_d(k) + \mu_d \frac{\partial J_{\text{LMAP}}(\mathbf{w}(k), y(k))}{\partial \mathbf{w}_d} \quad (26)$$

where

$$\frac{\partial J_{\text{LMAP}}(\mathbf{w}, y(k))}{\partial \mathbf{w}_d} = \frac{\sum_{p=2i-1}^{2i} \sum_{q=2l-1}^{2l} \exp\left(-\frac{|y(k) - s_{pq}|^2}{2\rho}\right) (s_{pq} - y(k))}{\sum_{p=2i-1}^{2i} \sum_{q=2l-1}^{2l} \exp\left(-\frac{|y(k) - s_{pq}|^2}{2\rho}\right)} \mathbf{r}^*(k) \quad (27)$$

and  $\mu_d$  is an adaptive gain. The choice of  $\rho$  should ensure a proper separation of the four clusters in  $S_{i,l}$ . If the value of  $\rho$  is too large, a desired degree of separation may not be achieved. On the other hand, if a too small  $\rho$  is used, the algorithm attempts to impose a very tight control in the size of clusters and may fail to do so. Apart from these two extreme cases, the performance of the algorithm does not critically depend on the value of  $\rho$ . As the minimum distance between the two neighbouring symbol points is 2, typically  $\rho$  is chosen to be less than 1.

Soft decision nature is evident in (27). Rather than committed to a single hard decision  $\mathcal{Q}[y(k)]$  as the DD scheme does, alternative decisions are also considered in a local region  $S_{i,l}$  that includes  $\mathcal{Q}[y(k)]$ , and each tentative decision is weighted by an exponential term  $\exp(\bullet)$  which is a function of the distance between the equalizer soft output  $y(k)$  and the tentative decision  $s_{pq}$ . This soft decision nature enables a simultaneous update of  $\mathbf{w}_c$  and  $\mathbf{w}_d$  without worrying error propagation and, therefore, simplifies the operation. It also has an effect that a larger adaptive gain  $\mu_d$  can often be used, compared with the DD scheme. It is also obvious that this SDD scheme corresponds to the last stage of the bootstrap MAP scheme given in [7],[8]. The complexity of the this CMA+SDD scheme is given in Table I, where it can be seen that computational complexity per weight update of this proposed new scheme is simpler than that of the CMA+DD scheme. The four  $\exp(\bullet)$  evaluations can be implemented through look up table in practice.

TABLE II  
A SIMULATED  $T_s/2$ -SPACED 22-TAP CHANNEL IMPULSE RESPONSE, WHERE  $T_s$   
DENOTES SYMBOL PERIOD.

Tap No.	Re	Im	Tap No.	Re	Im
0	0.0145	-0.0006	11	0.0294	-0.0049
1	0.0750	0.0176	12	-0.0181	0.0032
2	0.3951	0.0033	13	0.0091	0.0003
3	0.7491	-0.1718	14	-0.0038	-0.0023
4	0.1951	0.0972	15	0.0019	0.0027
5	-0.2856	0.1896	16	-0.0018	-0.0014
6	0.0575	-0.2096	17	0.0006	0.0003
7	0.0655	0.1139	18	0.0005	0.0000
8	-0.0825	-0.0424	19	-0.0008	-0.0001
9	0.0623	0.0085	20	0.0000	-0.0002
10	-0.0438	0.0034	21	0.0001	0.0006

### III. SIMULATION STUDY

The performance of the CMA+SDD and CMA+DD blind equalizers were evaluated in a computer simulation using the standard CMA blind equalizer as a benchmark. Two performance criteria were used to assess the convergence rate of a blind equalizer. The first one was a decision-based estimated MSE at each adaptation sample based on a block of  $N_{\text{MSE}} T_s$ -spaced data samples

$$\text{MSE} = \frac{1}{N_{\text{MSE}}} \sum_{k=1}^{N_{\text{MSE}}} |\mathcal{Q}[y(k)] - y(k)|^2. \quad (28)$$

The second one was the maximum distortion (MD) measure defined by

$$\text{MD} = \frac{\sum_{i=0}^{N_f-1} |f_i| - |f_{i_{\max}}|}{|f_{i_{\max}}|} \quad (29)$$

where  $\{f_i\}_{i=0}^{N_f-1}$  was the combined impulse response of the channel and equalizer defined by  $\bar{\mathbf{w}}^o \star \bar{\mathbf{a}}^e + \bar{\mathbf{w}}^e \star \bar{\mathbf{a}}^o$  with  $\star$  denoting convolution and  $N_f = N_c + m - 1$  being the length of the  $T_s$ -spaced combined impulse response, and

$$f_{i_{\max}} = \max\{f_i, 0 \leq i \leq N_f - 1\}. \quad (30)$$

The equalizer output signal constellation after convergence was also shown using  $N_{\text{test}} = 6000 T_s$ -spaced testing data samples not used in adaptation.

Extended simulation was performed but space limitation means that only a typical set of results can be presented. In the chosen simulated example, 256-QAM data symbols were transmitted through a  $T_s/2$ -spaced 22-tap channel whose CIR is given in Table II. The noise power was set to  $\sigma_e^2 = 4.24 \times 10^{-5}$ , corresponding to a channel signal to noise ratio of 60 dB. The  $T_s/2$ -spaced equalizer had 26 taps and the length of the data block for estimating the MSE at each adaptation was  $N_{\text{MSE}} = 1000$ . The adaptive gain for the CMA had to be set to  $\mu_c = 10^{-8}$  to avoid divergence. The two adaptive gains of the CMA+DD equalizer were set to  $\mu_c = 10^{-8}$  and  $\mu_d = 10^{-5}$ . For the CMA+SDD equalizer, the two adaptive gains were set to  $\mu_c = 10^{-8}$  and  $\mu_d = 2 \times 10^{-5}$  with a width  $\rho = 0.4$ . The equalizer length and all the adaptive algorithm parameters were chosen empirically to ensure fast convergence speed and good steady-state performance.

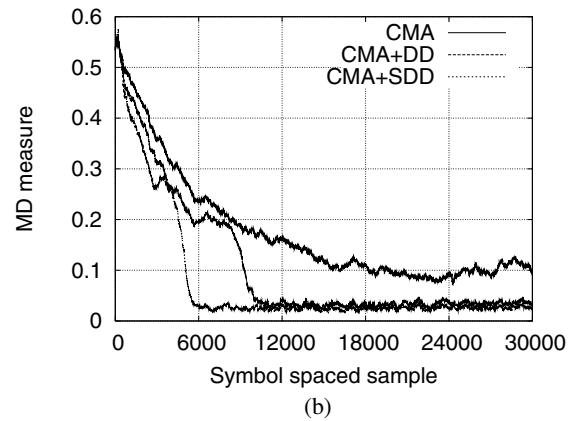
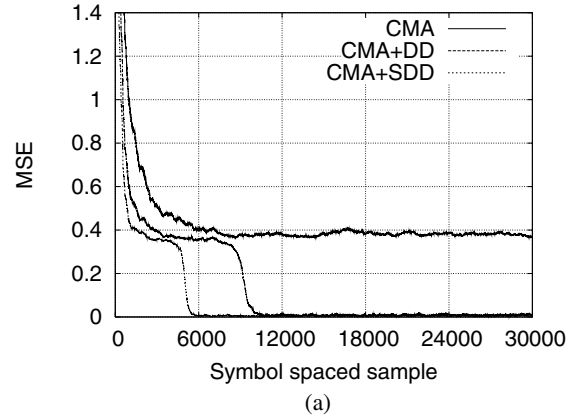


Fig. 4. Comparison of convergence performance in terms of (a) estimated MSE and (b) MD measure.

The learning curves of the three blind equalizers, in terms of the estimated MSE and MD measure, are depicted in Fig. 4 (a) and (b), respectively, while the equalizer output signal constellations after convergence are illustrated in Fig. 5. For this example, faster convergence speed of the proposed new scheme over the CMA+DD scheme can clearly be seen. The results also indicate that the steady-state equalization performance of the CMA+SDD algorithm is slightly better than the CMA+DD algorithm.

### IV. CONCLUSIONS

In this paper, a novel low-complexity blind equalization scheme has been proposed based on operating a CMA equalizer and a SDD equalizer concurrently. Compared with a state-of-art low-complexity blind equalization scheme, namely the recently introduced concurrent CMA and DD blind equalizer, the proposed concurrent CMA and SDD blind equalizer has simpler computational requirements, faster convergence rate and slightly better steady-state equalization performance. This new blind equalizer, together with the concurrent CMA and DD blind equalizer, offer practical alternatives to blind equalization of higher-order QAM channels and provide significant equalization improvement over the standard CMA based blind equalizer.

REFERENCES

- [1] D. Godard, "Self-recovering equalization and carrier tracking in two-dimensional data communication systems," *IEEE Trans. Communications*, Vol.COM-28, pp.1867–1875, 1980.
- [2] J.R. Treichler and B.G. Agee, "A new approach to multipath correction of constant modulus signals," *IEEE Trans. Acoustics, Speech and Signal Processing*, Vol.ASSP-31, No.2, pp.459–472, 1983.
- [3] J.R. Treichler, "Application of blind equalization techniques to voiceband and RF modems," in *Preprints 4th IFAC Int. Symposium Adaptive Systems in Control and Signal Processing (France)*, 1992, pp.705–713.
- [4] N.K. Jablon, "Joint blind equalization, carrier recovery, and timing recovery for high-order QAM signal constellations," *IEEE Trans. Signal Processing*, Vol.40, No.6, 1383–1398, 1992.
- [5] O. Macchi and E. Eweda, "Convergence analysis of self-adaptive equalizers," *IEEE Trans. Information Theory*, Vol.IT-3, No.2, pp.161–176, 1984.
- [6] F.C.C. De Castro, M.C.F. De Castro and D.S. Arantes, "Concurrent blind deconvolution for channel equalization," in *Proc. ICC'2001 (Helsinki, Finland)*, June 11-15, 2001, Vol.2, pp.366–371.
- [7] S. Chen, S. McLaughlin, P.M. Grant and B. Mulgrew, "Reduced-complexity multi-stage blind clustering equaliser," in *Proc. ICC'93 (Geneva, Switzerland)*, 1993, Vol.2, pp.1149–1153.
- [8] S. Chen, S. McLaughlin, P.M. Grant and B. Mulgrew, "Multi-stage blind clustering equaliser," *IEEE Trans. Communications*, Vol.43, No.3, pp.701–705, 1995.
- [9] J. Karaoguz and S.H. Ardalan, "A soft decision-directed blind equalization algorithm applied to equalization of mobile communication channels," in *Proc. ICC'92 (Chicago, U.S.A.)*, 1992, Vol.3, pp.343.4.1–343.4.5.
- [10] S. Chen, T.B. Cook and L.C. Anderson, "Blind FIR equalisation for high-order QAM signalling," in *Proc. 6th Int. Conf. Signal Processing (Beijing, China)*, Aug.26-30, 2002, pp.1299–1302.
- [11] S. Chen, T.B. Cook and L.C. Anderson, "A comparative study of two blind FIR equalizers," *Digital Signal Processing*, Vol.14, pp.18–36, 2004.
- [12] R. Johnson, Jr., P. Schniter, T.J. Endres, J.D. Behm, D.R. Brown and R.A. Casas, "Blind equalization using the constant modulus criterion: a review," *Proc. IEEE*, Vol.86, No.10, pp.1927–1950, 1998.

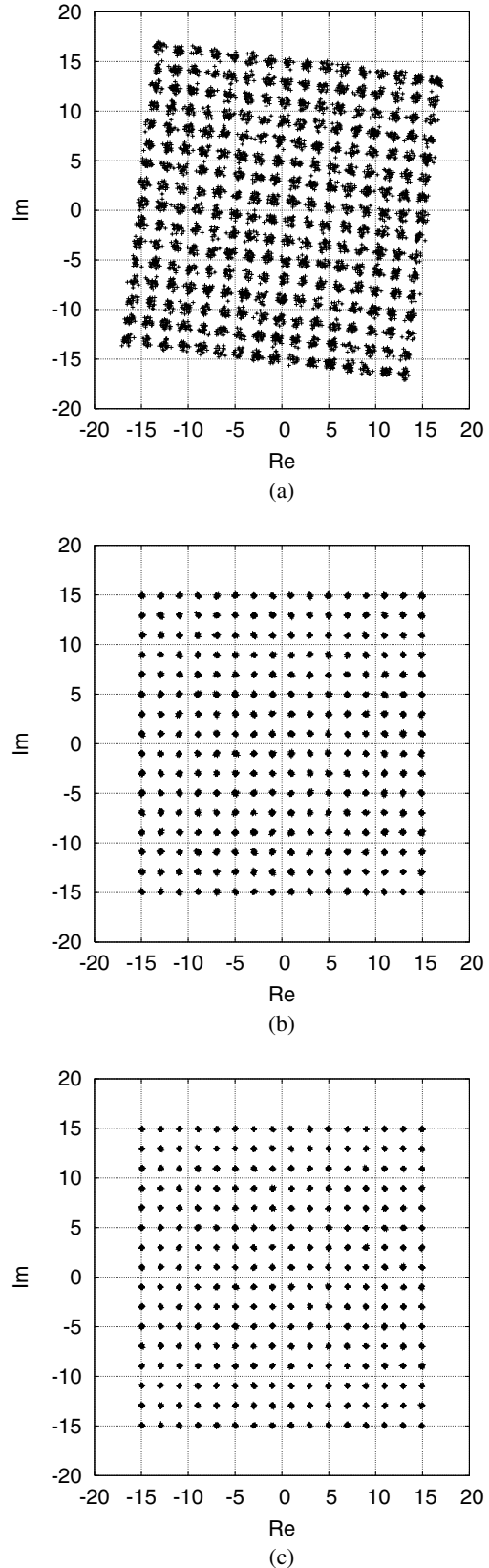


Fig. 5. Equalizer output signal constellations after convergence (a) the CMA, (b) the CMA+DD, and (c) CMA+SDD.